



## Two new polyketides from Hawaiian endophytic fungus *Pestalotiopsis* sp. FT172

Chunshun Li<sup>a,b</sup>, Ariel M. Sarotti<sup>c</sup>, Wesley Yoshida<sup>d</sup>, Shugeng Cao<sup>a,b,\*</sup>

<sup>a</sup>Department of Pharmaceutical Sciences, Daniel K. Inouye College of Pharmacy, University of Hawaii at Hilo, 200 West Kawili Street, Hilo, HI 96720, United States

<sup>b</sup>Cancer Biology Program, University of Hawaii Cancer Center, 701 Ilalo Street, Honolulu, HI 96813, United States

<sup>c</sup>Instituto de Química Rosario (CONICET), Facultad de Ciencias Bioquímicas y Farmacéuticas, Universidad Nacional de Rosario, Suipacha 531, Rosario 2000, Argentina

<sup>d</sup>Chemistry Department, University of Hawaii at Manoa, 2545 The Mall, Honolulu, HI 96822, United States

### ARTICLE INFO

#### Article history:

Received 19 October 2017

Revised 18 November 2017

Accepted 20 November 2017

Available online 22 November 2017

#### Keywords:

Endophytic fungi

Hawaii

*Pestalotiopsis*

FT172

NMR

Mosher reaction

### ABSTRACT

Two new polyketides, pestalotiotones A (**1**) and B (**2**) were isolated from the cultured broth of *Pestalotiopsis* sp. FT172. The structures of compounds **1** and **2** were determined by analysis of HRMS and NMR spectroscopic data. The absolute configurations of compound **1** were assigned by Mosher reaction, *J*-based configuration analysis, and DP4 NMR calculations. Both compounds were tested against cancer cell lines, pathogenic fungi and bacteria.

© 2017 Elsevier Ltd. All rights reserved.

Polyketides with C<sub>3</sub> moieties are formally biosynthesized through the polyketide pathway from C-3 modules, which are found in different organisms including bacteria, fungi, insects, and marine molluscs.<sup>1–5</sup> Some of the polyketides with C<sub>3</sub> moieties have been totally synthesized because of their unique structures and various activities.<sup>6–9</sup> During our continuing investigation of bioactive compounds from Hawaiian plant derived fungi,<sup>10–19</sup> eight ambuic acid derivatives were isolated from an endophytic fungus *Pestalotiopsis* sp. FT172.<sup>15</sup> Further investigation of the cultured broth enabled us to isolate two new polyketide metabolites, pestalotiotones A (**1**) and B (**2**)<sup>20</sup> (Fig. 1), each with multiple C<sub>3</sub> units.

Compound **1**<sup>20d</sup> was isolated as gum. Its molecular formula, C<sub>22</sub>H<sub>36</sub>O<sub>5</sub>, was determined by HRESIMS at *m/z* 381.2637 [M+H]<sup>+</sup> (calcd 381.2636), requiring five degrees of unsaturation. Comprehensive analysis of the 1D and 2D NMR spectra (Table 1) indicated the presence of seven methyls, two methylenes, eight methines (including two olefinic, two oxygenated), and five carbons with no hydrogen attached. Two spin systems, 19–7–8 and 21–11 (10)–12–13(22)–14–15(23)–16–17, were established by the

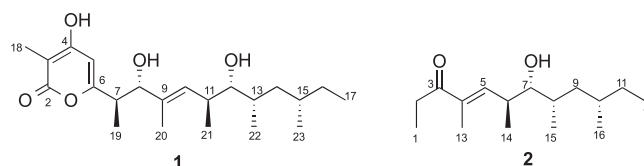


Fig. 1. Structure of compounds **1** and **2**.

<sup>1</sup>H–<sup>1</sup>H COSY spectrum as shown in Fig. 2, which was also verified by the corresponding HMBC correlations (Fig. 2).

Besides, the HMBC correlations from singlet methyl (H<sub>3</sub>-20, δ<sub>H</sub> 1.65) to the olefinic carbons C-9 and C-10, and the oxygenated methine C-8 (δ<sub>C</sub> 81.0) established the aliphatic chain from C-7 all the way to C-17. Furthermore, HMBC correlations from the olefinic methine (δ<sub>H</sub> 6.06, H-5) to the oxygenated olefinic or carbonyl carbons δ<sub>C</sub>169.8 (C-4) and δ<sub>C</sub>166.1 (C-6), and from the methyl singlet (H<sub>3</sub>-18, δ<sub>H</sub> 1.84) to C-2 (δ<sub>C</sub> 169.5), C-3 (δ<sub>C</sub> 98.8), and C-4 (δ<sub>C</sub>169.8) implied the presence of the 3-methyl-4-hydroxy-pyran-2-one moiety. Meanwhile, the observed HMBC cross-peaks from H-5 to C-7, and from the methyl doublet (H<sub>3</sub>-19) to C-6, C-7 and C-8 suggested the connection of the aliphatic chain to C-6 of the pyranone moiety through C-7. Then, the planar structure of compound **1** was elucidated as shown. The configuration of the double bond at C9–C10 was assigned to be *E* by the NOE correlations from H-10 to

\* Corresponding author at: Department of Pharmaceutical Sciences, Daniel K. Inouye College of Pharmacy, University of Hawaii at Hilo, 200 West Kawili Street, Hilo, HI 96720, United States.

E-mail address: [scao@hawaii.edu](mailto:scao@hawaii.edu) (S. Cao).

**Table 1**  
NMR Spectroscopic Data for **1** and **2** in MeOH  $d_4$ .

No.	<b>1</b>		<b>2</b>	
	$^1\text{H}^a$	$^{13}\text{C}^{b}$	$^1\text{H}^a$	$^{13}\text{C}^{b}$
1			1.06, t, 7.4	9.37
2		169.5	2.74, dq, 14.6, 7.4	31.2
3		98.8		205.3
4		169.8		137.2
5	6.06, s	103.1	6.79, dd, 9.7, 1.5	147.5
6	–	166.1	2.81, m	38.3
7	2.67, m	43.6	3.30, m	79.1
8	4.10, d, 9.7	81.0	1.64, m	34.6
9		136.1	1.35, m	42.0
			0.95, m	
10	5.40, d, 9.4	134.5	1.46, m	32.5
11	2.62, m	37.0	1.35, m	29.8
			1.03, m	
12	3.20, dd, 8.1, 4.0	79.1	0.84, t, 7.4	11.3
13	1.73, m	33.4	1.77, d, 1.4	11.7
14	1.42, m	42.6	1.01, d, 6.9	17.2
	0.97, m			
15	1.44, m	32.6	0.90, d, 6.7	14.9
16	1.36, m	30.3	0.87, d, 6.6	20.2
	1.08, m			
17	0.87, t, 5.7	11.6		
18	1.84, s	8.4		
19	1.03, d, 7.1	16.2		
20	1.65, d, 1.3	11.0		
21	0.91, d, 6.8	17.9		
22	0.88, d, 7.0	14.2		
23	0.86, d, 7.3	20.1		

<sup>a</sup> Spectra recorded at 500 MHz.

<sup>b</sup> Spectra recorded at 125 MHz. Data based on  $^1\text{H}$ ,  $^{13}\text{C}$ , HSQC, and HMBC experiments.

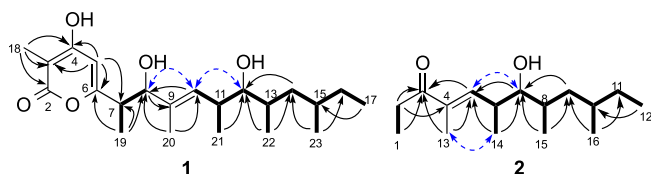


**Fig. 2.** COSY (Bold), key HMBC (Single headed) and NOESY (Double headed dash) correlations of **1**.

H-8 and H-12. The absolute configurations of compound **1** were determined by Mosher reaction,  $J$ -based configuration analysis, as well as DP4 NMR calculations.

In order to determine the absolute configuration of C-8 and C-12, compound **1** was reacted with  $R$ - and  $S$ -Mosher reagents.<sup>21</sup> The results showed that compound **1** should have an  $S$  and  $R$  configuration at 8- and 12-position, respectively (Fig. 3).

With the absolute configurations at C-8 and C-12 determined, we next carried out a  $J$ -based configuration analysis to determine the configuration of 7-, 11-, 13-, and 15-positions.<sup>22</sup> For the 1,2-

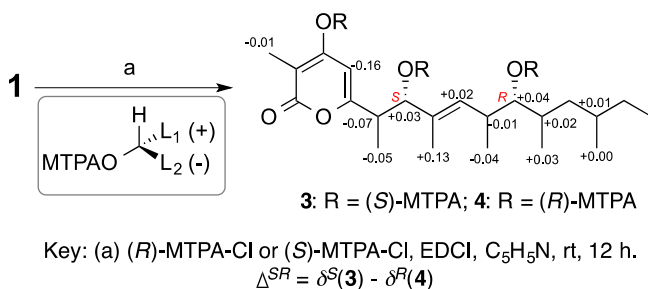


**Fig. 3.** Reactions of compound **1** with Mosher esters.

methine system at C7-8, both  $^3J_{\text{H-7,H-8}}$  (9.4 Hz) and  $^2J_{\text{H-7,C-8}}$  (–6.7 Hz) values indicated the *anti* configuration for H-7/H-8. However, the data could not be used to distinguish between the two possible rotamers *threo* A-3 and *erythro* B-3, so instead an NOE experiment (Fig. 4) was carried out. Irradiation of the H<sub>3</sub>-19 signal resulted in the enhancement of H<sub>3</sub>-20, which was evidence for only the *erythro* B-3 rotamer. For the C11-12 methine system a medium coupling constant ( $^3J_{\text{H-11,H-12}} = 6.9$  Hz) indicated that alternating conformers were present in solution. Additional coupling constants ( $^2J_{\text{H-11,C-12}} = -5.2$  Hz, large;  $^3J_{\text{H-12,C-10}} = 1.3$  Hz, small) showed that only the *erythro* B-1, B-3 rotamers were present (Fig. 4). Hence, the relative

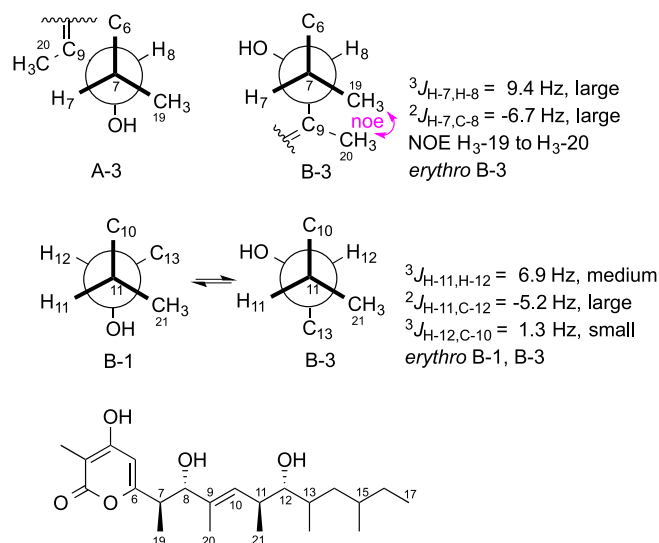


**Fig. 4.**  $J$ -based configuration analysis for the configuration of compound **1** at C-7, C-8, C-11 and C-12.

stereochemistry of the C7-8 and C11-12 portions of the molecule was determined by applying *J*-based configuration analysis. However, the experimental NMR data collected for **1** precluded the unequivocal *J*-based configurational analysis at C-13 and C-15.

In order to overcome this limitation, we undertook quantum calculations of NMR shifts, a useful strategy for the structural elucidation of complex organic molecules,<sup>23</sup> extensively used by us in the elucidation process of a wide plethora of natural products derived from Hawaiian plants.<sup>16–19</sup> Among the different strategies that have been developed for the correlation between experimental and calculated NMR data, the DP4 probability (developed by the Goodman group)<sup>24</sup> and the updated DP4+ version (developed by the Sarotti group)<sup>25</sup> emerge as the most popular methods for stereochemical assignment when only one set of experimental NMR data is available.<sup>23a</sup> One of the major differences between both methodologies is the level of theory employed during the geometry optimization stage (generally, the most time-demanding step in the overall NMR calculation procedure): MMFF in the case of DP4, and B3LYP/6-31G\* in the case of DP4+. For that reason, and taking into consideration the size and conformational flexibility of the present system, we decided to use the DP4 method. Since the configurations at C-8, C-9, C-11 and C-12 were determined by well-known experimental procedures, we focused our attention on the stereochemistry at the remaining centers (C-13 and C-15), leading to four possible diastereoisomers (compounds **1a–d**, Fig. 5). Following the original procedure, exhaustive conformational searches of the target compounds were carried out at the MMFF level, and NMR calculations of all conformers located within a 10 kcal/mol window in each case were performed at the B3LYP/6-31G\*\* level of theory (see Supporting Information). As shown in Fig. 5, the DP4 calculations identified isomers **1a** (~66%) and **1c** (~34%) as the most likely candidates. Noticeably, both compounds display the opposite configuration at the remote C-15 position, therefore suggesting that the C-11/C-13 stereotriad should be *anti-syn*. We also noticed high errors in the NMR predictions of C-3 and C-4 in all cases ( $\Delta\delta \sim 8.8$  and 13.4 ppm, respectively), which is a typical situation in related systems with possible tautomerism.<sup>23b</sup> Nevertheless, the DP4 recomputed by removing these conflicting resonances afforded almost the same preference towards **1a** and **1c** (~65% and ~35%, respectively). Hence, according to our experimental and computational results herein described, the most likely structure of pestalotiotone A should be **1a**, featuring a stereoheptad with 7*R*,8*S*,11*S*,12*R*,13*S*,15*S* configuration.

Compound **2**<sup>20e</sup> was isolated as gum. The positive HRESIMS quasi-molecular ion peak at  $m/z$  255.2314  $[M+H]^+$  (calcd 255.2319) suggested the molecular formula of **2** as C<sub>16</sub>H<sub>30</sub>O<sub>2</sub>, with two degrees of unsaturation. The <sup>1</sup>H, <sup>13</sup>C and the HSQC NMR spectra (Table 1) indicated the presence of six methyls, three methylenes, five methines (including one olefinic, one oxygenated), and two quaternaries including one ketone ( $\delta_C$  205.3) and one olefinic

( $\delta_C$  137.2) carbon. <sup>1</sup>H–<sup>1</sup>H COSY spectrum indicated the presence of two spin systems, 1–2 and 5–6 (14)–7–8(15)–9–10(16)–11–12, which were also verified by the corresponding HMBC correlations (Fig. 2). Furthermore, the observed HMBC correlations from the methyl groups H<sub>3</sub>-1 and H<sub>3</sub>-13, and the only olefinic proton H-5 to the ketone ( $\delta_C$  205.3), and from H<sub>2</sub>-2 and H<sub>3</sub>-13 to olefinic quaternary carbon C-4 undoubtedly connected the two spin systems. The configuration of the double bond at C4-C5 was determined to be *E* by the NOE correlations between H-5 and H-7, as well as H<sub>3</sub>-13 and H<sub>3</sub>-14.

Biogenetically, compound **2** could be the immediate precursor of compound **1**. Hence, the configuration at 6-, 7-, 8-, and 10-positions of compound **2** was suggested to be the same as 11-, 12-, 13-, and 15-positions of compound **1**, respectively, based on their NMR similarity and the same sign of optical rotation. However, in order to reinforce our assignment, we carried out NMR calculations at the B3LYP/6-31G\*\*//MMFF level of theory of the four possible isomers of **2** with a C-6/C-7 *anti* relationship (Fig. 6). In good agreement with our computational findings discussed above for **1**, isomer **2a**, which features the *anti-syn-syn* stereotetrad, was identified as the most likely isomer in high confidence (~84%).

Moreover, **1** and **2** are very similar to a group of compounds called pestalpolyols A–I.<sup>5,26,27</sup> The structure of pestalpolyol A, which was unambiguously assigned by single-crystal X-ray diffraction analysis,<sup>5</sup> has the same side chain as determined for **1** (Fig. 7). Interestingly, the reported NMR data for pestalpolyol A, which was derived from one acetyl-CoA, nine malonyl-CoA and eight L-methionine,<sup>27</sup> matched nicely with our experimental findings for **1** and **2** at the analogous positions, providing further evidence

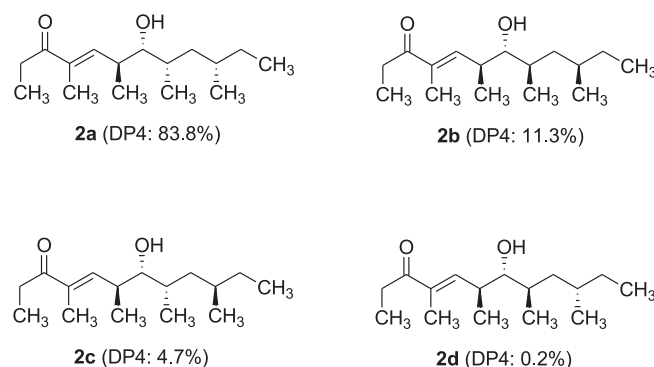


Fig. 6. Isomers of **2** considered for DP4 calculations.

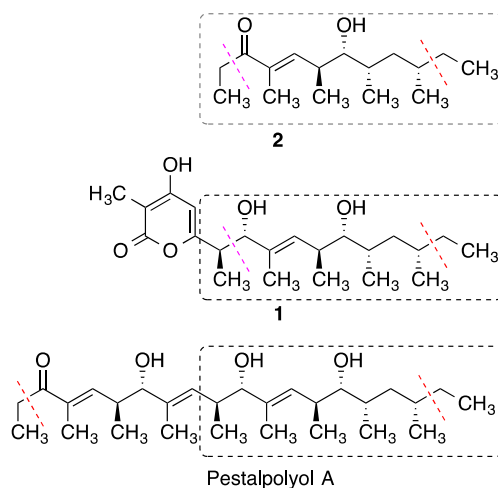


Fig. 7. Structural similarity of **1** and **2** to pestalpolyol A.

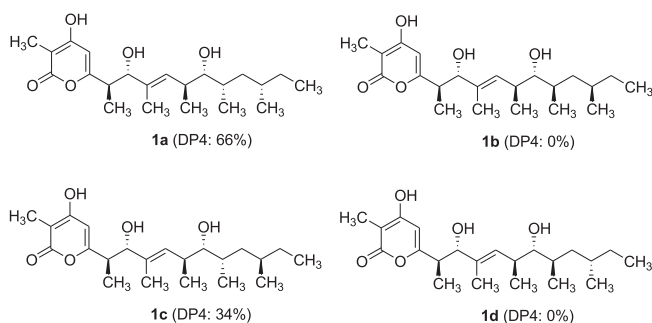


Fig. 5. Isomers of **1** considered for DP4 calculations.

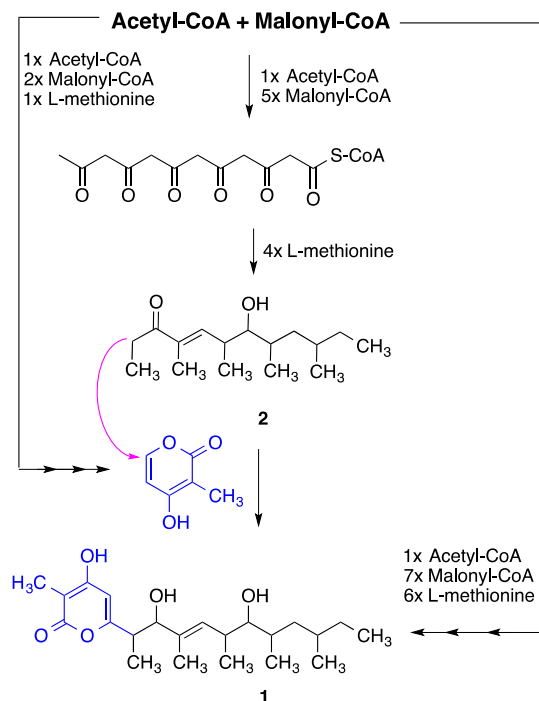


Fig. 8. Proposed biosynthesis of compounds 1 and 2.

in our stereoassignment based on Mosher reaction, *J*-based configuration analysis, and NMR calculations.

Like pestalpolyols A–I, biosynthetically compounds 1 and 2 could be derived from the polyketide pathway (Fig. 8).<sup>27</sup> Compound 2 was derived from one acetyl-CoA, five malonyl-CoA and four L-methionine. Nucleophilic reaction between compound 2 and 4-hydroxy-3-methyl-2H-pyran-2-one yields compound 1. Alternatively, compound 1 could also be directly derived from one acetyl-CoA, seven malonyl-CoAs and six L-methionines.

Compounds 1 and 2 were tested against cancer cell lines A2780 and A2780CisR,<sup>28</sup> but both were not active. Compounds 1 and 2 were also evaluated against four bacterial strains *Escherichia coli*, *Pseudomonas aeruginosa*, *Staphylococcus aureus*, and *Bacillus subtilis*, and four fungal strains *Penicillium chrysogenum*, *Aspergillus niger*, *Paecilomyces lilacinus*, and *Fusarium graminearum* for their antibacterial and anti-fungal activities,<sup>29</sup> but neither was active.

### Conflict of interest

Notes: The authors declare no competing financial interest.

### Acknowledgments

This work was financially supported mainly by a start-up funding from Daniel K. Inouye College of Pharmacy (DKICP), University of Hawaii at Hilo (UHH), and the Victoria S. and Bradley L. Geist Foundation, Hawaii, United States (15ADVC-74420 and 17CON-86295) (to SC). We also thank Ms Xiaohua Wu (DKICP, UHH) for her help in the anti-proliferative assay.

### A. Supplementary data

Supplementary data associated with this article can be found, in the online version, at <https://doi.org/10.1016/j.tetlet.2017.11.045>.

### References

- Davies-Coleman MT, Garson MJ. *Nat Prod Rep.* 1998;15:477–493.
- Pankewitz F, Hilker M. *Biol Rev.* 2008;83:209–226.
- Paul MC, Zubia E, Ortega MJ, Salva J. *Tetrahedron.* 1997;53:2303–2308.
- Zhao LX, Huang SX, Tang SK, et al. *J Nat Prod.* 2011;74:1990–1995.
- Li J, Xie J, Yang YH, Li XL, Zeng Y, Zhao PJ. *Planta Med.* 2015;81:1285–1289.
- Cutignano A, Villani G, Fontana A. *Org Lett.* 2012;14:992–995.
- Magnin-Lachaux M, Tan Z, Liang B, Negishi E. *Org Lett.* 2004;6:1425–1427.
- Miller AK, Byun DH, Beaudry CM, Trauner D. *PNAS.* 2004;101:12019–12023.
- Masamune S, Abiko A. *Tetrahedron Lett.* 1996;37:1081–1084.
- Li CS, Yang BJ, Fenstemacher R, Turkson J, Cao S. *Tetrahedron Lett.* 2015;56:1724–1727.
- Li CS, Ding Y, Yang BJ, et al. *Org Lett.* 2015;17:3556–3559.
- Li CS, Ding Y, Yang BJ, Yin H-Q, Turkson J, Cao S. *Phytochemistry.* 2016;126:41–46.
- Li CS, Ren G, Yang B, et al. *Org Lett.* 2016;18:2335–2338.
- Fei-Zhang DJ, Li CS, Cao S. *Cancer Biol Ther.* 2016;17:709–712.
- Li CS, Yang B, Turkson J, Cao S. *Phytochemistry.* 2017;140:77–82.
- Li CS, Sarotti AM, Turkson J, Cao S. *Tetrahedron Lett.* 2017;58:2290–2293.
- Huang P, Li CS, Sarotti AM, Turkson J, Cao S. *Tetrahedron Lett.* 2017;58:1330–1333.
- Li CS, Sarotti AM, Yang B, Turkson J, Cao S. *Molecules.* 2017;22(7), pii:E1166.
- Li CS, Sarotti AM, Huang P, et al. *Sci Rep.* 2017;7:10424.
- (a) *General experimental procedures:* Optical rotations were measured with a Rudolph Research Analytical AutoPol IV Automatic Polarimeter. UV and IR spectra were obtained with Shimadzu UV-1800 spectrophotometer and Thermo scientific Nicolet iS50FT-IR spectrometer, respectively. NMR spectra including 1D and 2D experiments were recorded in methanol-*d*<sub>4</sub> on a Varian Unity Inova 500 MHz and Bruker 400 MHz. High resolution mass spectra were obtained on an Agilent Q-ToF Ultima ESI-TOF mass spectrometer. HPLC was carried out on Agilent 1100 LC system, and all solvents were HPLC grade. Column chromatography used Diaion HP-20.
- (b) *Strain isolation and cultivation:* The isolation, identification and fermentation of the fungal strain *Pestalotiopsis* sp. FT172 was reported in our previous paper.<sup>15</sup>
- (c) *Extraction and isolation:* The fermented whole broth (5 L) was filtered through filter paper to separate the supernatant from the mycelia. The former was passed through HP-20 eluted with MeOH-H<sub>2</sub>O (10%, 30%, 50%, 70%, 90%) to afford five fractions (Fr. A–E). The Fr. E (720.0 mg) was separated by preparative HPLC (C18 column, 5  $\mu$ ; 100.0 mm  $\times$  21.2 mm; 15 mL/min, 20–100% MeOH/H<sub>2</sub>O in 30 min, followed by 100% MeOH in 10 min) to produce 40 sub-fractions (SF. 1–40). The sub-fraction SF.26 (6.19 mg) was subjected to the semi-preparative HPLC (C18 column, 5  $\mu$ ; 250.0 mm  $\times$  10.0 mm; 3 mL/min; with 0.1% formic acid in 45% MeCN/H<sub>2</sub>O) to yield compound 2 (1.21 mg, *t*<sub>R</sub> 23.2 min). SF. 27 (5.42 mg) was purified by semi-preparative HPLC (Phenyl-Hexyl column, 5  $\mu$ ; 250.0 mm  $\times$  10.0 mm; 3 mL/min; with 0.1% formic acid in 42% MeCN/H<sub>2</sub>O) to yield compound 1 (1.28 mg, *t*<sub>R</sub> 23.2 min).
- (d) *Pestalotiote A (1):* yellowish gum;  $[\alpha]_D^{25} +33.6$  (*c* = 0.05, MeOH); UV (MeOH)  $\lambda_{max}$  (log  $\epsilon$ ) 204 (4.18), 289 (3.59) nm; IR  $\nu_{max}$  3378, 2960, 2928, 2873, 1652, 1589, 1500, 1456, 1416, 1375, 1358, 1251, 1169, 1083, 1043, 1012, 995  $cm^{-1}$ ; <sup>1</sup>H (in methanol-*d*<sub>4</sub> at 500 MHz, and in CDCl<sub>3</sub> at 400 MHz) and <sup>13</sup>C NMR (in methanol-*d*<sub>4</sub>, 125 MHz) data, see Table 1; positive HR-ESIMS *m/z* 381.2637 [M+H]<sup>+</sup> (calcd for C<sub>22</sub>H<sub>37</sub>O<sub>6</sub> 381.2636).
- (e) *Pestalotiote B (2):* yellowish gum;  $[\alpha]_D^{25} +28.4$  (*c* = 0.02, MeOH); UV (MeOH)  $\lambda_{max}$  (log  $\epsilon$ ) 231 (3.76) nm; IR  $\nu_{max}$  3417, 2960, 2927, 2874, 1659, 1652, 1590, 1460, 1377, 1353, 1261, 1216, 1046  $cm^{-1}$ ; <sup>1</sup>H (in methanol-*d*<sub>4</sub> at 500 MHz, and in CDCl<sub>3</sub> at 400 MHz) and <sup>13</sup>C NMR (in methanol-*d*<sub>4</sub>, 125 MHz) data, see Table 1; positive HR-ESIMS *m/z* 255.2314 [M+H]<sup>+</sup> (calcd for C<sub>16</sub>H<sub>31</sub>O<sub>2</sub> 255.2319).
- Cao S, Guza RC, Wisse JH, Miller JS, Evans R, Kingston DG. *J Nat Prod.* 2005;68:487–492.
- Matsumori N, Kaneno D, Murata M, Nakamura H, Tachibana K. *J Org Chem.* 1999;64:866–876.
- (a) Grimblat N, Sarotti AM. *Chem Eur J.* 2016;22:12246–12261; (b) Lodewyk MW, Siebert MR, Tantillo DJ. *Chem Rev.* 2012;112:1839–1862; (c) Zanardi MM, Suárez AG, Sarotti AM. *J Org Chem.* 2017;82:1873–1879; (d) Zanardi MM, Sarotti AM. *J Org Chem.* 2015;80:9371–9378.
- Smith SG, Goodman JM. *J Am Chem Soc.* 2010;132:12946–12959.
- Grimblat N, Zanardi MM, Sarotti AM. *J Org Chem.* 2015;80:12526–12534.
- Xie J, Li J, Yang YH, Li XN, Chen YH, Zhao PJ. *Arch Pharm Res.* 2015;1–6.
- Perez Hemphill CF, Daletos G, Liu Z, Lin W, Proksch P. *Tetrahedron Lett.* 2016;57:2078–2083.
- (a) Anti-proliferative Assays: Viability of A2780 cells was determined using the CyQuant assay according to the manufacturer's instructions (Life Technologies, CA, USA). Briefly, cells were cultured in 96-well plates at 1000 cells per well for 24 h and subsequently treated with compounds (20  $\mu$ g/mL) for 72 h and analyzed. Relative viability of the treated cells was normalized to the DMSO-treated control cells. 17a,b Delazar A, Byres M, Gibbons S, et al. Iridoid glycosides from *Eremostachys glabra*. *J Nat Prod.* 2004;67:1584–1587; (b) Sridhar C, Subbaraju GV, Venkateswarlu Y, Venugopal RT. *J Nat Prod.* 2004;67:2012–2016.
- Shen CC, Syu WJ, Li SY, Lin CH, Lee GH, Sun CM. *J Nat Prod.* 2002;65:1857–1862.